The Journal of Molecular Diagnostics, Vol. 18, No. 2, March 2016

ELSEVIER

the Journal of Molecular Diagnostics

jmd.amjpathol.org

Quantitative Detection and Resolution of *BRAF* V600 Status in Colorectal Cancer Using Droplet Digital PCR and a Novel Wild-Type Negative Assay

Roza Bidshahri,* Dean Attali,† Kareem Fakhfakh,* Kelly McNeil,‡ Aly Karsan,‡ Jennifer R. Won,§ Robert Wolber,¶ Jennifer Bryan,† Curtis Hughesman,* and Charles Haynes*

From the Michael Smith Laboratories, Department of Statistics,† and the Canadian Immunohistochemistry Quality Control Unit,§ Department of Pathology and Laboratory Medicine, University of British Columbia, Vancouver; the Department of Genetics and Molecular Diagnostics,‡ British Columbia Cancer Agency, Vancouver; and the Department of Pathology,¶ Lion's Gate Hospital, North Vancouver, British Columbia, Canada*

Accepted for publication September 17, 2015.

Address reprint requests to Charles Haynes, Ph.D., Canada Research Chair in Interfacial Biotechnology, University of British Columbia, Vancouver, BC V6T 1Z4; or Curtis Hughesman, Ph.D., Michael Smith Laboratories, University of British Columbia, Vancouver, BC V6T 1Z4. E-mail: israels@chbe.ubc.ca or curtish@msl.ubc.ca.

A need exists for robust and cost-effective assays to detect a single or small set of actionable point mutations, or a complete set of clinically informative mutant alleles. Knowledge of these mutations can be used to alert the clinician to a rare mutation that might necessitate more aggressive clinical monitoring or a personalized course of treatment. An example is *BRAF*, a (proto)oncogene susceptible to either common or rare mutations in codon V600 and adjacent codons. We report a diagnostic technology that leverages the unique capabilities of droplet digital PCR to achieve not only accurate and sensitive detection of $BRAF^{V600E}$ but also all known somatic point mutations within the *BRAF* V600 codon. The simple and inexpensive two-well droplet digital PCR assay uses a chimeric locked nucleic acid/DNA probe against wild-type *BRAF* and a novel wild-type–negative screening paradigm. The assay shows complete diagnostic accuracy when applied to formalin-fixed, paraffin-embedded tumor specimens from metastatic colorectal cancer patients deficient for Mut L homologue-1. *(J Mol Diagn 2016, 18: 190–204; http://dx.doi.org/10.1016/j.jmoldx.2015.09.003)*

Somatic variations within (proto)oncogenes and key signaling pathways are screened in cancer testing laboratories to refine disease diagnoses and to enable targeted approaches to therapy.[1–3] Detection of somatic point mutations (SPMs) in exons 19 and 21 of the gene encoding epidermal growth factor receptor (EGFR), for example, is used to establish the therapeutic value of EGFR tyrosine kinase inhibitors in treating non-small cell lung cancer,[4] whereas SPMs within codons 12 and 13 of *KRAS* are theranostic of response to anti-EGFR antibody-based treatment of colorectal cancer (CRC).[5] For these and many other clinically actionable genes, one of the various forms of allele-specific (AS) or mutation-specific PCR is often used to detect somatic variants within a single codon or adjacent codons.[6–10] Alternatively, an immunohistochemical (IHC) staining assay may be used to detect the resulting amino acid substitution(s) within the gene product.[11] In either case, the assays are generally designed to detect a specific SPM or a limited set of SPMs, even in instances in which a larger number of mutations in the target oncogene are known to occur and to be of clinical significance. In comparison, examples of PCR-based assays designed to detect all known mutant (MT) alleles within an oncogene are rare. They generally use nested AS primers, substantial multiplexing, and a relatively large number of reaction wells.[12] The assays are therefore relatively complex in structure.

Alternatively, comprehensive somatic variant analysis may be achieved by next-generation sequencing (NGS),

Supported by Genome Canada Strategic Opportunity Fund grant SOF151 and National Sciences and Engineering Research Council of Canada Discovery grant 311796 (both to C.H.).

Disclosures: None declared.

http://dx.doi.org/10.1016/j.jmoldx.2015.09.003

which is expected to find increasing use in clinical testing of patients as the sensitivity of the method improves, and as the cost and throughput of the technology become increasingly more manageable to health care providers.[13–15] Several bench-top NGS instruments suitable for targeted molecular diagnostics are now available for clinical use. Large repositories and panels of primers have been assembled (eg, AmpliSeq, TruSeq) to enable preparation of amplicon libraries that target oncogenic hot-spot regions that are frequently mutated.[16,17] In response to these growing capabilities, governments, health care providers, and payers are actively working toward defining NGS usage in clinical tests, with current updates for reimbursement through the Protecting Access to Medicare Act (Genetic Tests for Cancer Diagnosis: *http://www.cms.gov/medicare-coverage-database*, last accessed May 1, 2013) suggesting health insurers in the United States are poised to decline reimbursements for sequencing-based somatic profiling in the absence of evidence that i) clinically actionable genomic alterations are (likely) present in the specimen; ii) the quality and quantity of the genomic DNA (gDNA) recovered from the specimen are sufficiently high, particularly if it is a formalin-fixed, paraffin-embedded (FFPE) sample; and iii) the frequency of the mutation(s) is great enough to permit reliable sequence analysis. Current targeted resequencing methods generally offer a mutant frequency (MF) detection limit (LOD) of approximately 5% to 10%, but projected advances in NGS and associated bioinformatics suggest this LOD can be reduced to levels, at least in theory, approaching 1% MF.[18,19] Although clearly an improvement, the higher depths of sequencing required will likely decrease NGS throughput, and a sensitivity of 1% MF still remains above the sensitivity that can be obtained in PCR-based assays. We are therefore developing the tools needed to create sensitive and robust AS probe-based droplet-digital PCR (ddPCR) assays that clinics may use as a simple and inexpensive stand-alone method to define proper courses of therapy through comprehensive profiling of somatic variations in oncogene(s) present in either FFPE specimens or circulating tumor DNA. Assays developed with the platform may also serve as a way of rapidly and cheaply identifying patients for whom acquisition of further sequencing data are justified.

The activating V600E mutation in exon 15 of the v-raf murine sarcoma viral oncogene homolog B1 gene (*BRAF*) on human chromosome 7q34 is present in approximately 40% to 60% of advanced melanomas,[20,21] 40% to 80% of papillary thyroid cancers, and approximately 50% of CRCs exhibiting Mut L homologue-1 (MLH1)-associated microsatellite instability.[22,23] *BRAF* encodes the serine-threonine protein kinase B-Raf associated with the mitogen-activated protein kinase pathway regulating cell expansion, differentiation, and apoptosis. Food and Drug Administration-approved therapeutics for $BRAF^{V600E}$-positive metastatic or unresectable melanomas that lack evidence of activating mutations in downstream effectors include the MT B-Raf inhibitors PLX4032 (vemurafenib; Roche, Basel, Switzerland) and Tafinlar (dabrafenib; GlaxoSmithKline, Brentford, UK).[24,25] Either small molecule binds the active state of the kinase domain to selectively inhibit the proliferation of cells with unregulated B-Raf activity. Resistance to vemurafenib or dabrafenib often occurs within 6 to 12 months, necessitating careful disease monitoring.[26] When relapse is observed, the Food and Drug Administration has approved treatment of $BRAF^{V600E}$-positive patients with the use of a combination of dabrafenib and the mitogen-activated protein kinase extracellular signal-related kinase kinase inhibitor trametinib; that regimen is also approved for treating $BRAF^{V600K}$-positive metastatic or unresectable melanomas.[27] In addition to V600E (79% to 84% of all V600 coding mutations) and V600K (8% to 12%), V600R (2% to 5%), V600M (0.3% to 4%), V600D (0.3% to 1.3%), V600G (approximately 1.3%), V600A (<1%), and V600L (<1%) mutations are observed, and there is evidence that V600 mutation status correlates with metastasis-free survival and may be associated with other distinct oncologic features of melanoma.[28–30] Importantly, there is increasing evidence that B-Raf and mitogen-activated protein kinase extracellular signal-related kinase kinase inhibitors can be effective in treating late-stage melanoma patients harboring any nonsynonymous *BRAF* V600 mutation.[31]

National Comprehensive Cancer Network clinical practice guidelines for colorectal cancer (*http://www.nccn.org/professionals/physician_gls/f_guidelines.asp*, last accessed August 25, 2015) also recommend *BRAF* mutational testing of MLH1-deficient CRC patients, because the antitumor activity of anti-EGFR antibodies (cetuximab, panitumumab) may be suppressed or lost in $BRAF^{V600E}$-positive patients.[32] Moreover, the $BRAF^{V600E}$ mutation correlates well with adverse pathologic features and distinct clinical characteristics of CRC,[33,34] including altered differentiation mucinous histology, microsatellite instability, and CpG (-C-phosphate-G-) island methylator phenotype. As with melanoma, other $BRAF^{V600}$ mutations are observed in CRC, with the total collective incidence of nonsynonymous V600 mutations estimated at 10% to 15%, including an approximately 50% to 60% freqency in MLH1-deficient CRCs.[35]

BRAF status is also being considered as a prognostic biomarker for papillary thyroid cancer, because disease progression and reoccurrence correlate substantially with $BRAF^{V600E}$.[36] Correct identification of V600 status is therefore integral to understanding and treating cancers in which B-Raf activity plays an important role. A clinical pipeline that permits rapid, accurate, and sensitive detection of $BRAF^{V600E}$ and tumors that harbor a rare nonsynonymous V600 mutation at a frequency suitable for NGS analysis could serve to improve clinical and pathologic staging to achieve better management of *BRAF*-related cancers.

We report here a diagnostic technology that leverages the unique capabilities of ddPCR to rapidly and effectively discriminate patients carrying wild-type (WT) *BRAF* from those carrying a $BRAF^{V600E}$ mutation or any other V600

mutation. Nearest-neighbor type molecular thermodynamic models developed in our laboratory[37,38] are used to design a locked nucleic acid (LNA) substituted dual-labeled hydrolysis probe against *BRAF*^{V600E1} (Val600Glu c.1799t>a) to quantitatively detect that clinically relevant somatic variation. Those models and a corresponding model for unsubstituted DNA[39] are also used to optimize two dual-labeled hydrolysis probes against WT *BRAF* over the hot-spot oncogenic region within codons 598 to 603: one in a standard pure-DNA format and the other a LNA/DNA chimera. Either of these WT-specific probes is expected to show sufficiently low cross-reactivity to any known V600 mutation that MT and WT alleles can be unequivocally discriminated. We show that this essential capability is not provided by the standard pure-DNA probe but is fully realized by the LNA-substituted probe when applied in a ddPCR format. A second LNA-substituted probe that targets a highly conserved 16-nt sequence within *BRAF* is used to quantify the total number of amplifiable *BRAF* templates within the gDNA sample, permitting the MF to be quantified with high accuracy to a LOD of 0.05% while also defining the total quantity of amplifiable DNA present in the sample. The method offers advantages over either AS/mutation-specific PCR or IHC assays through its sensitivity to all *BRAF* V600 mutations; it likewise holds advantages over high-resolution melt analysis, particularly when applied to genomic DNA recovered from FFPE samples, by not only detecting the presence of a mutation but also quantifying the MF and the mass of high-quality amplifiable DNA present in the sample; two variables essential to properly assessing the potential success of a subsequent NGS run and the depth of sequencing that would be required. The performance of this novel ddPCR *BRAF* V600 status assay is demonstrated through successive application first to a set of plasmid-DNA standards, each presenting a specific V600 MT allele, over a range of MT frequencies, and then to sets of reference cell lines and FFPE tissues. Finally, clinical utility is assessed by comparing results from our ddPCR *BRAF* V600 status assay to those from a validated *BRAF*^{V600E} IHC assay when applied to FFPE tumor specimens from 41 CRC patients positive for microsatellite instability.

Materials and Methods

Oligonucleotides

All primers, pure-DNA and LNA-substituted dual-labeled hydrolysis probes, and WT and MT *BRAF* alleles were purchased from IDT, Inc. (Coralville, IA). Probes were purified by high-performance liquid chromatography, whereas primers and templates were purified by desalting. Purified primers, probes, and templates were resuspended to 100 μmol/L in IDTE (10 mmol/L Tris, pH 8.0, 0.1 mmol/L EDTA) buffer and stored at −20°C before use.

Primers and Probes Design

Forward and reverse primers (Table 1) were designed with the use of Primer3.[40] Primers used to amplify a 165-bp fragment that spanned across the V600 codon were designed within the *BRAF* intron/exon 15 boundary. All primers were analyzed by primer-BLAST to find any sequence similarities within the human genome database.[41]

Each dual-labeled hydrolysis probe (Table 1) was likewise engineered to minimize PCR artifacts and to selectively hybridize to a specific sequence within *BRAF* at ddPCR reaction conditions. The consensus probe, a 16-nucleotide (nt) 6-carboxyfluorescein (FAM) or hexachloro-fluorescein (HEX)-labeled/Black-Hole Quencher 1-quenched probe that spanned *BRAF* codons 607 to 612, was designed using the melting thermodynamics model of Hughesman et al[37] to define the combinations of LNA substitutions needed to limit probe length to within a highly conserved region of exon 15 and to achieve a melting temperature (T_m) of approximately 66°C to 67°C when duplexed to WT *BRAF*. That model accounts for the effects of PCR solution conditions and the addition of a fluorescent reporter dye (HEX or FAM) and quencher (Black-Hole Quencher 1) on probe-template melting thermodynamics. Potential probe-derived PCR artifacts were identified and avoided with primer-Blast software.[42] The LNA *BRAF* V600 WT-specific probe and the LNA *BRAF*^{V600E1}-specific probe that spanned *BRAF* hot-spot codons 598 to 603 were designed in a similar manner. There, however, the LNA-DNA mismatch thermodynamics model of Hughesman et al[38] was used to identify probe sequences that minimize probe cross-reactivity to nontarget alleles. Finally, a 23-nt pure-DNA version of the WT-specific probe was designed as a benchmark for evaluating the performance improvements conferred by LNA substitutions. Melting thermodynamics required for WT-specific DNA probe design were predicted with a corresponding melting thermodynamic model developed by Hughesman et al[39] for unsubstituted DNA duplexes.

Model predicted T_m values for probes were verified experimentally by UV melt spectroscopy according to standard methods.[41]

Tumor and Reference Samples, and DNA Extraction Protocols

FFPE tissues from a cohort of metastatic CRC patients were obtained from Lion's Gate Hospital (North Vancouver, BC, Canada) with approval from the University of British Columbia Clinical Ethics Research Board number H14-00577. The CRC cases were selected from a pool of MLH1-deficient tumors, identified by IHC testing as part of the population-based Vancouver Coastal Health Lynch syndrome screening program. Three non−MLH1-deficient cases (no. 3, no. 5, and no. 20) were also included. Specimens were derived from 10% neutral-buffered formalin-fixed resections in all but one case (no. 37), which was a

Table 1 Sequences and Concentrations of Primers and Dual-labeled Hydrolysis Probes Used in the ddPCR *BRAF* V600 Status Assay

Primer/Probe	Sequence	Concentration (μM)
Forward primer	5′-CTACTGTTTTCCTTTACTTACTACACCTCAGA-3′	0.9
Reverse primer	5′-AGCCTCAATTCTTACCATCCA-3′	0.9
LNA V600E$_1$-specific probe	5′-(6-FAM)/AGATTTCTCTGTAGC/(BHQ_1)-3′	0.25
Consensus probe*	(HEX)/TCCCATCAG/ZEN/TTTGAACAGTTGTCTGG/(IABkFQ)	0.25

Locked nucleic acid of base type are underlined.
*Consensus probe labeled with HEX in well 1 and 6-FAM in well 2.
6-FAM™, 6-carboxyfluorescein; HEX™, hexachloro-fluorescein; BHQ_1, Black Hole Quencher® 1; ZEN, Internal Quencher; IABkFQ, Iowa Black FQ.

formalin-fixed specimen of malignant ascites fluid. The original diagnosis was confirmed by a pathologist (R.W.), and an optimal tumor block that contained invasive carcinoma was selected for sampling. Two cores of each carcinoma were taken for construction of tumor microarray blocks, and two additional cores were taken for PCR studies. Four FFPE standards, each harboring either WT *BRAF* or a verified frequency of a particular V600 MT allele (0.8% V600K MF, 1.4% V600E, or 50% V600R), were purchased from Horizon Discovery Ltd. (Cambridge, UK). DNA from FFPE reference standards and CRC FFPE cores was purified with the use of the QIAamp DNA FFPE tissue kit (Qiagen, Inc., Santa Clarita, CA) under a modified protocol for the xylene-assisted paraffin removal step that serves to reduce shearing of genomic DNA during that process. Xylene (0.8 mL) was added to FFPE cores (two) collected in 1.5-mL microcentrifuge tube, and the mixture was equilibrated by rotational mixing for 10 minutes. The sample was then centrifuged at 12,500 × *g* for 1 minute to collect tissue. The waste xylene was removed, and the process was repeated twice more. Three successive washes with 0.8 mL of 100%, 100%, and 70% ethanol, respectively, were then completed with the same procedure. Finally, the sample was placed in a Vacufuge (Eppendorf, Hamburg, Germany) for 5 minutes at medium heat to dry, and the residue was carefully removed for further processing according to the standard QIAamp DNA FFPE protocol.

Purified gDNA from the SW480 cell line (WT *BRAF*) and the YUMAC cell line (homozygous for *BRAF*^{V600K}) was kindly provided by the BC Cancer Agency. pIDTSMART-AMP plasmids, each containing a 280-bp gene fragment (exon 15) of either WT *BRAF* or a *BRAF* V600 MT allele, were purchased from IDT, Inc.

DNA concentration was measured with a NanoDrop ND-1000 spectrophotometer (Thermo Scientific, Waltham, MA). Because plasmids exhibit supercoiling, pIDTSMART plasmid DNA (1.5 μg) was linearized with ClaI restriction enzyme according to the manufacturer's instructions (Life Technologies; Carlsbad, CA) before concentration determination and use in assays.

ddPCR Assay Workflow and Characterization

Digital PCR mastermix solutions (20 μL) were prepared from 2× dUTP-free ddPCR supermix for probes (Bio-Rad, Inc., Hercules, CA), 900 nmol/L each of the forward and reverse primers, 250 nmol/L of the consensus probe, 250 nmol/L of either the LNA *BRAF*^{V600E1} probe (well 1) or the LNA *BRAF* V600 WT-specific probe or pure-DNA *BRAF* V600 WT-specific probe (well 2), and an amount of purified plasmid or gDNA that contained approximately 10,000 copies of *BRAF* [gDNA purified from clinical colorectal FFPE samples sometimes contained fewer copies (approximately 5000 to 8000) of amplifiable *BRAF*]. No template control samples were prepared in IDTE buffer. Emulsified sub-nanoliter reaction droplets were created by introducing a 20-μL sample into a well of an eight-channel disposable DG8 droplet generator cartridge and adding 60 μL of droplet generation oil (Bio-Rad Inc.). Forty microliters of the resulting droplet emulsion (approximately 13,000 to 15,000 droplets) generated on the Bio-Rad QX-100 Droplet Generator were transferred by multichannel p100 pipette to an Eppendorf Twin.tec semiskirted 96-well PCR plate, which was then heat-sealed with foil sheets. The droplet emulsions were thermally cycled in a CFX96 thermocycler with the use of the following protocol: denaturation at 95°C for 10 minutes, followed by 50 cycles of 94°C for 30 seconds and 60°C for 1 minute (ramp rate set to 2.5°C/second). The end-point fluorescence of each thermally cycled droplet was measured with a QX100 Droplet Reader (Bio-Rad Inc.). After cycling, a final 10-minute hold at 98°C was applied to deactivate the enzyme and to stabilize the droplets. The raw ddPCR data were collected and visualized with the QuantaSoft software version 1.2 (Bio-Rad Inc.). MF values were then determined from droplet counts either through operator-based assignment of MT and WT data clusters (hereafter referred to as the manual method) or with the use of an automated data analysis algorithm described in the *Results* section.

Serial dilutions (1000 to 1 copies/μL) of the WT *BRAF* isolated from plasmid DNA, as well as each of 10 different MT *BRAF* alleles, were prepared in IDTE buffer (IDT, Inc.), with the concentration of *BRAF* template (in copies/uL) in each dilution quantified on a Bio-Rad QX100 ddPCR instrument. For dynamic-range measurements, 1000 to 1 copies/μL of BRAF V600 MT plasmid-derived DNA was prepared in a high fixed background (10,000 copies per μL) of WT *BRAF* plasmid DNA. Serial dilutions (1000 to 1 copies per μL) of *BRAF*^{V600K} gDNA from YUMAC cells and *BRAF*^{V600K} (YUMAC cells) in WT *BRAF* (SW480 cells) were prepared in the same manner.

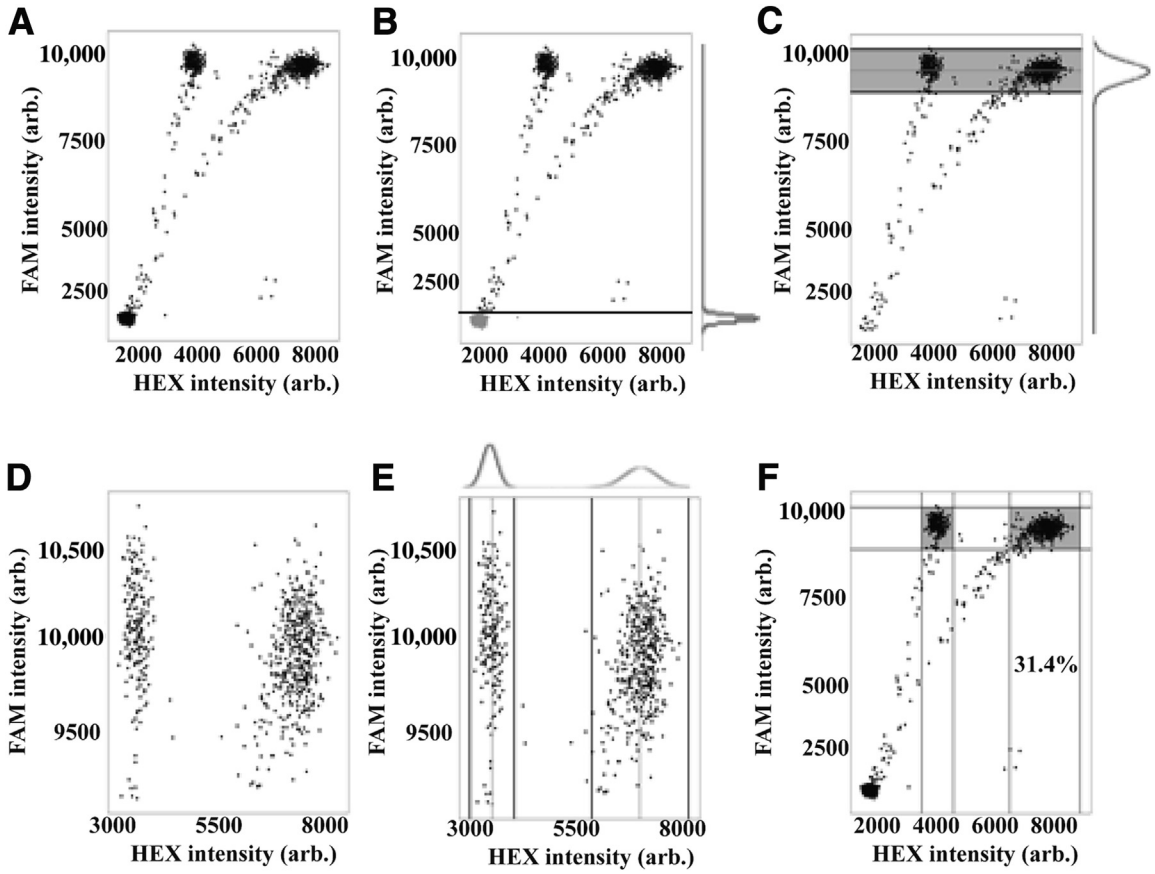

Figure 1 *BRAF* V600 status assay automated data analysis overview. **A:** Representative output data for the WT-negative portion (well) of the assay are visualized in a two-dimensional scatter plot. **B** and **C:** Empty droplets (marked as gray dots) are identified by fitting to the FAM channel signal two normal distributions, one of low mean intensity (**B**) and the other of high mean intensity (**C**). All droplets (**B**) below a threshold FAM intensity (**black line**) set at the mean of the lower-intensity distribution plus 7 SDs are deemed empty and removed from the analysis. All filled droplets are then identified (**C**) as lying within the means ± 3 SDs of the upper distribution (**gray band**). **D:** Droplets displaying FAM intensities outside this range (often referred to as digital PCR rain) are taken as being poor in signal quality and excluded from the analysis. **E:** *BRAF* V600 WT^- and WT^+ droplets, respectively, are identified by fitting two normal distributions to the HEX channel signal, with the relevant populations bound by the means ± 3 SDs in each case. The distribution having the lower mean HEX intensity contains the population of WT-negative droplets. **F:** Analysis of the original data in **A** defines the populations of WT^- (**left gray box**) and WT^+ (**right gray box**) droplets, from which the mutant frequency is calculated as the ratio of WT^- droplets to total droplets (ie, 195/(195 + 426) × 100 = 31.4%). Arb, arbitrary; FAM, 6-carboxyfluorescein; HEX, hexachlorofluorescein; WT, wild-type.

ddPCR Raw Data Analysis Algorithm

The droplet event data are exported from QuantaSoft software version 1.3.2 (Bio-Rad, Inc.) into custom software we developed that analyzes the data to assign each read droplet as either empty, rain (droplets having a signal lying within an indeterminate region between a pair of distinct positive and negative droplet clusters), MT^+, or WT^+. The assigned droplets are then used to detect MT alleles and compute the MF in each well. The software was built in the R version 3.2.2 programing language (*https://www.r-project.org*, last accessed August 25, 2015) and is available on GitHub (*https://github.com/daattali/ddpcr*, last accessed August 25, 2015) along with a detailed description of its features and computational elements. An illustration of the data analysis process and a brief overview of the core computational steps of the algorithm are provided in Figure 1.[43]

B-Raf V600E MT-Specific Antibody Staining

The CRC tumor microarray was cut at 4-μm thick sections for IHC studies. Deparaffinized sections were stained on a Ventana (Tucson, AZ) Benchmark XT automated immunostainer with the use of a 32-minute CC1 heat-induced antigen retrieval protocol. Incubation with VE-1 mouse monoclonal primary antibody (Spring Biosciences, Pleasanton, CA) directed against $B\text{-}Raf^{V600E}$ protein was for 16 minutes at 37°C. Antibody was detected with the Ventana Optiview system with the use of diaminobenzidine as a chromogen. Previous experience with this antibody suggested that homogeneous cytoplasmic staining of carcinoma cells indicates the presence of B-Raf V600E protein. Nonspecific nuclear staining, readily distinguished from cytoplasmic staining, was encountered in both benign and malignant colorectal epithelium in some cases. Blinded IHC

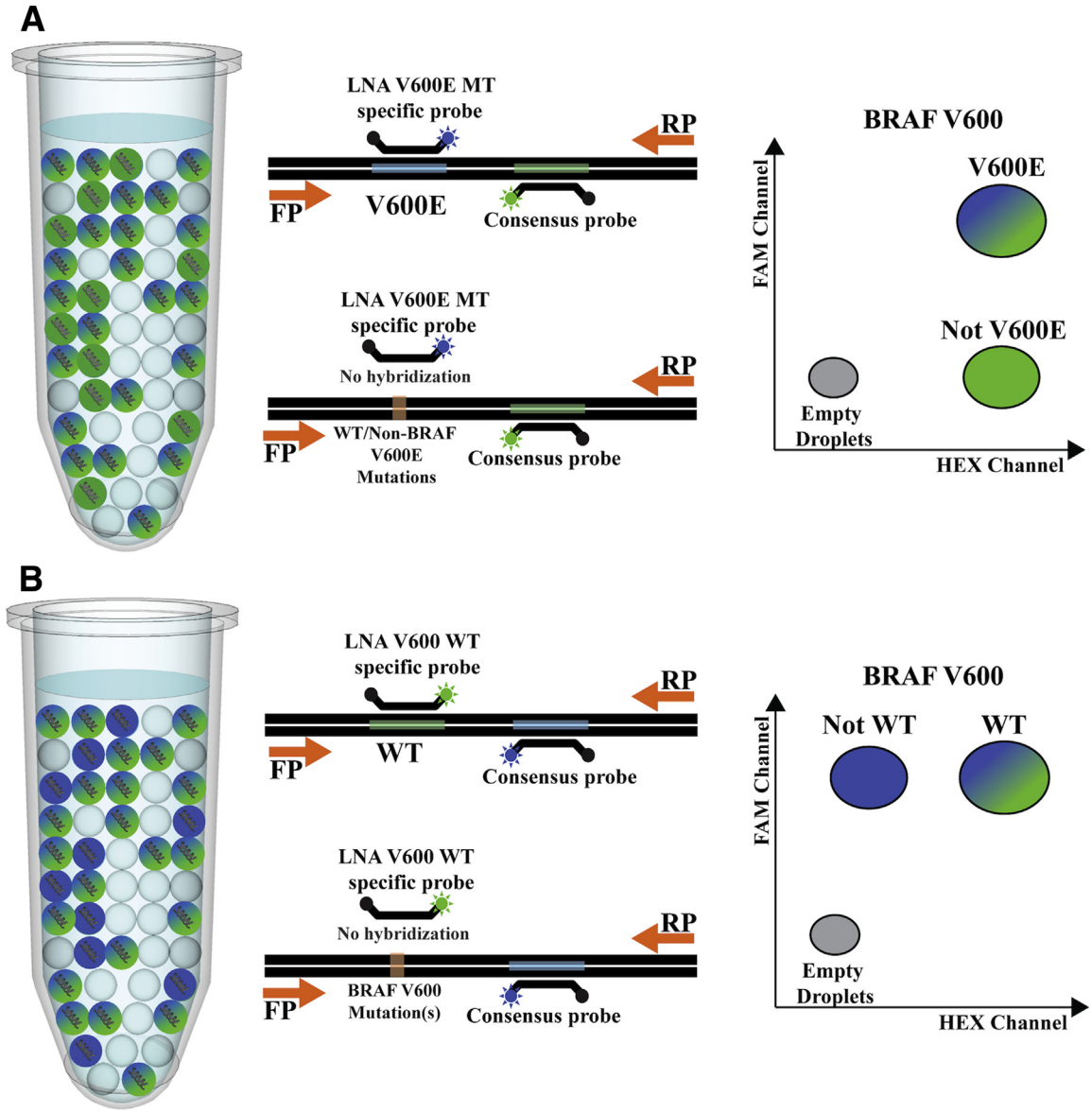

Figure 2 Schematic of the ddPCR *BRAF* V600 status assay for identifying WT, V600E1, and less common *BRAF* V600 MT alleles in CRC tumor samples. Water-in-oil emulsion droplets are generated to contain digital PCR mix and a small aliquot of genomic DNA that contains, on average 0.2 to 0.4 CPD *BRAF* allele(s). The two-well assay uses forward and reverse primers that amplify a 165-bp fragment of the *BRAF* gene that spans codon V600. Two dual-labeled hydrolysis probes that span *BRAF* codons 598 to 603 are used. **A:** The first, used in well 1, is a HEX-labeled LNA-substituted probe designed to selectively hybridize and unequivocally detect $BRAF^{V600E1}$ by showing no cross-reactivity to other clinically relevant *BRAF* alleles. **B:** The second, used in well 2, is a FAM-labeled probe designed to hybridize only to WT *BRAF* and thereby distinguish WT V600 from all *BRAF* V600 MT alleles. A consensus probe that binds to a highly conserved sequence within the *BRAF* amplification template is also added to each reaction well. With the use of well 2 as an illustration of assay mechanics, when a *BRAF* V600 WT allele (**upper duplex** of **B**) is amplified, end-point fluorescence signals from the WT-specific probe (green) and the consensus probe (blue) are both detected. Amplification of any *BRAF* V600 MT allele (**lower duplex** of **B**) results in the generation of an end-point signal from the consensus probe only. In the resulting ddPCR two-dimensional plot (output data), droplets that contain amplicons of a V600 WT allele cluster in the FAM^{+}/HEX^{+} quadrant (**top right**), whereas droplets that contain those of V600 MT allele cluster in the FAM^{+}/HEX^{-} quadrant (**top left**). Droplets that contain no *BRAF* template cluster in the **bottom left** (FAM^{-}/HEX^{-}) quadrant. CPD, copies per droplet; CRC, colorectal cancer; ddPCR, droplet-digital PCR; FAM, 6-carboxyfluorescein; FP, forward primer; HEX, hexachloro-fluorescein; LNA, locked nucleic acid; MT, mutant; RP, revers primer; WT, wild-type.

scoring was performed by two pathologists (R.W. and Brandon Sheffield) and a histotechnologist (Deanna Johnson) over a multiheaded microscope. Tumor microarray cases scored as indeterminate were retested by IHC on the whole section from which the corresponding tumor microarray core was taken and then rescored.

Results

Assay Design and the Unique Advantages of ddPCR

Our assay of *BRAF* V600 status is a two-well test that uses ddPCR for target amplification and detection. In both wells,

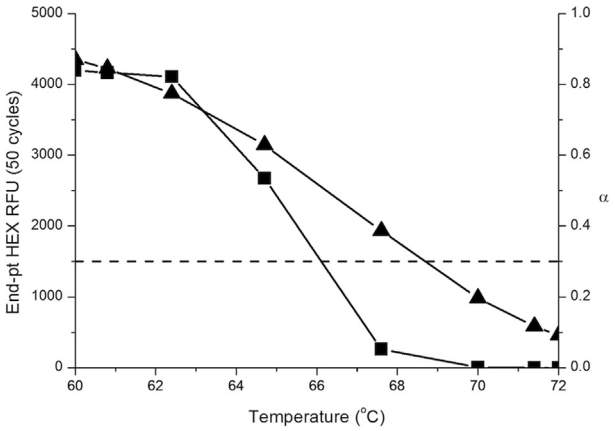

Figure 3 General relation between the end-point fluorescence (**squares**; **left** *y* axis) and the fraction α of template bearing a dual-hydrolysis probe (**triangles**; **right** *y* axis) as a function of the PCR annealing temperature T_a. Data reported for end-point fluorescence monitoring of qPCR amplification of WT *BRAF* (plasmid; $C_T = 0.5$ μmol/L) with the use of the LNA V600 WT-specific probe (Table 1). Data points represent mean values for triplicate runs at each T_a, with the size of the data points commensurate with the SD for the data point having the largest experimental error. HEX, hexachloro-fluorescein; LNA, locked nucleic acid; qPCR, quantitative real-time PCR; RFU, relative fluorescence unit; WT, wild-type.

gDNA purified from an FFPE tissue specimen is loaded to a copies per drop of 0.2 ± 0.05, ensuring that at the start of the PCR most droplets contain either 0 or 1 copy of a *BRAF* gene. Approximately 10,000 copies of *BRAF* are analyzed per test. Well 1 (Figure 2A) also contains ddPCR supermix for probes without dUTP (Bio-Rad Inc.) and primers and two dual-hydrolysis probes whose sequences and labeling chemistries are reported in Table 1. The resulting amplicons (WT and MT) are 165 bp in length, spanning most of *BRAF* exon 5, including codons 598 to 603. During amplification, fluorescence generated from hydrolysis of the *BRAF* consensus probe confirms the presence of a *BRAF* gene (WT or MT) in the droplet, allowing the total amplifiable copies of *BRAF* in the specimen to be quantified by HEX^+ droplet counts and Poisson statistics.

Well 1 also contains a $BRAF^{V600E1}$ MT-specific probe that is model-designed (see *Engineering Allele Specificity into Probes Used in ddPCR Assays*) to contain a pattern of LNA substitutions that ensures sufficiently low cross-reaction of the probe to WT *BRAF* or other V600 MT alleles at ddPCR conditions to avoid overlap of $BRAF^{V600E1}$ and non-$V600E_1$ data fields. Droplets clustered in the HEX^+/FAM^+ quadrant therefore unambiguously quantify $BRAF^{V600E1}$ alleles, whereas those displaying a HEX^+/FAM^- signal quantify all WT plus non-$V600E_1$ alleles, from which the frequency of $BRAF^{V600E1}$ within the specimen may be quantified. Well 1 therefore is a standard AS/mutation-specific PCR assay that targets and quantifies a MT allele ($BRAF^{V600E1}$) within a high background of WT allele. It is conducted here in a ddPCR format, but other studies have shown that it can also be effectively performed in a standard quantitative real-time PCR format with the use of either an AS primer or an AS probe, often in the presence of blocking agents that minimize cross-reactivity.[44]

In the second well (Figure 2B), our novel WT^- screen is applied to the gDNA sample to collectively detect and quantify all *BRAF* V600 mutations. The *BRAF* consensus probe, now FAM labeled, functions as described in the previous paragraph. The second probe (Table 1) is designed to selectively hybridize only WT *BRAF* and to thereby discriminate WT *BRAF* (FAM^+/HEX^+ signal) from any *BRAF* allele that carries a V600 mutation (FAM^+/HEX^- signal). In both wells, droplets that recorded a HEX^-/FAM^- signal contain no *BRAF*. Digital PCR offers capabilities essential to effective execution of the WT-negative screen. To fix ideas, consider a gDNA specimen that harbors 10,000 total copies of *BRAF*, 10% of which are a MT *BRAF* allele and the remainder WT *BRAF*. In the WT-negative screen, the probe targets the WT allele. If the screen were conducted in a quantitative real-time PCR format, the decrease in copies of WT *BRAF* from 10,000 (no MT alleles) to 9000 (10% MT frequency) would, in theory, result in a C_q (quantitation cycle) change of approximately 0.1, which cannot be measured with statistical significance (ΔC_q errors in AS PCR assays are typically approximately ± 0.3). Conversely, when the WT-negative assay is conducted in a ddPCR format, templates are partitioned into individual droplets, enabling droplets that contain WT *BRAF* to be fully differentiated from those that contain MT *BRAF* through their end-point HEX intensities. Small populations of MT *BRAF* may thereby be reliably detected and quantified.

Together, the combined ddPCR output from the two wells permits unequivocal stratification of tumors bearing WT *BRAF* from those carrying either $BRAF^{V600E1}$ or a rare V600 mutation. It also provides values for MF and the total abundance of amplifiable *BRAF*.

Engineering Allele Specificity into Probes Used in ddPCR Assays

In addition to the unique capabilities offered by ddPCR, successful execution of the two-well *BRAF* V600 status assay described in Figure 1 requires the two probes against the *BRAF* V600 region to be sufficiently specific to their target allele that cross-reactivity at PCR conditions does not diminish assay performance. Designing a real-time probe to unequivocally discriminate a target allele from an ensemble of alleles that may differ from the target sequence by as little as a single base is, in part, a problem rooted in chemical equilibria. Taking design of the probe against WT *BRAF* V600 (Figure 2B) as an example, it requires creating sufficient difference [$\Delta T_{m,WT-MT_i}$] between $T_{m,WT}$, the T_m of the perfectly matched duplex formed by the probe and its WT target, and $\Delta T_{m,MT_i}$, the T_m for the mismatched duplex formed by the probe and any MT allele *i*. In particular, $T_{m,WT}$ must exceed T_a, the annealing temperature of the PCR assay, such

Table 2 Experimental and Model-Predicted $\Delta T_{m,WT-MT_i}$ Values for Mismatched Duplexes Formed between a *BRAF* V600 MT Allele and Either a Pure-DNA or an LNA-Substituted V600 WT-Specific Probes Shown in Table 1

BRAF V600 Mutation (i)		Mismatch	Prevalence (%)	DNA WT V600 probe $\Delta T_{m,WT-MT_i}$ (°C)			LNA WT V600 probe $\Delta T_{m,WT-MT_i}$ (°C)		
				Pred*	Expt†	α‡	Pred	Expt	α
V600E$_1$	c.1799 t>a	A/A	79.0–84.0	4.3	4.2	0.85	11.8	11.0	<0.01
V600E$_2$	c.1799_1800 tg > aa	CA/AA		§	8.5			23.9	
V600K	c.1798_1799 gt > aa	AC/AA	8.0–12.4		7.4			23.8	
V600R	c.1798_1799 gt > ag	AC/AG	2.2–5.0		6.6			18.5	
V600M	c.1798g > a	C/A	0.14–4	4.6	6.2	0.69	12.0	14.1	<0.01
V600D	c.1799_1800 tg > at	CA/AT	0.3–1.3		8.6			24.7	
V600G	c.1799 t > g	A/G	0–1.3	1.9	1.4	0.89	7.7	7.6	0.21
V600L$_1$	c.1798 g > c	C/C	0–0.29	7.6	7.4	0.27	16.9	17.8	<0.01
V600L$_2$	c.1798 g > t	C/T	NA	5.1	6.6	0.63	12.6	15.4	<0.01
V600A	c.1799 t > c	A/C	NA	4.9	4.6	0.66	12.0	11.6	<0.01

*Pred $\Delta T_{m,WT-MT_i}$ determined for a C_T = 0.5 μmol/L (probe + allele; 50 mmol/L KCl, 3 mmol/L Mg^{2+}) with DNA mismatch corrections determined with the use of variables of SantaLucia et al[50] with LNA mismatches determined by $\Delta\Delta G_{LNA:MM}$ variables of Hughesman et al.[39]

†Expt $\Delta T_{m,WT-MT_i}$ determined by UVM analysis at a C_T = 2 μmol/L in buffer that contained 50 mmol/L KCl and 3 mmol/L Mg^{2+}.

‡α values computed for single mismatched base pairs with the use of $\Delta G_{MT_i}(T_a)$ values computed with the use of the method of Hughesman et al.[39]

§Current models[39] not valid for predicting tandem DNA-DNA or LNA-DNA mismatches. Also reported are prevalence data for *BRAF* V600 somatic mutations in melanoma[20–22] and α values for V600 MT alleles bearing a single point mutation.

Expt, experimental; LNA, locked nucleic acid; MT, mutant; NA, no data available; Pred, predicted; WT, wild-type.

that the duplex formed between the probe and WT template is sufficiently stable that creation of each WT amplicon results in hydrolysis of the bound probe and reporter release. $\Delta T_{m,MT_i}$ must then be low enough that concurrent amplification of any MT allele i at T_a results in a negligible signal from the WT-specific probe over the course of the ddPCR run. If melting heat capacity effects, which are small,[37] are ignored, the fraction α of MT template i to which a WT-specific probe is hybridized at T_a can be estimated from the thermodynamic relation as follows:

$$\ln\left(\frac{C_T(1-\alpha)^2}{2\alpha}\right) = -\frac{\Delta G_{MT_i}(T_a)}{RT_a} \quad (1)$$

Where $\Delta G_{MT_i}(T_a)$ is the Gibbs energy change for the melting transition at T_a and C_T is the total strand concentration, probe plus allele. The above equation shows that the value of α is a metric of the cross-reactivity of the probe; moreover, through its dependence on $\Delta G_{MT_i}(T_a)$, α also provides an indication of the stability of the duplex formed between the probe and MT template i. Previous real-time PCR studies have qualitatively shown that probe efficiency (fraction of amplification events that result in probe hydrolysis) decreases with decreasing stability of the probe:template duplex.[45] Our results, an example of which is shown in Figure 3, indicate that the dependence of probe efficiency on duplex stability causes the end-point fluorescence in a real-time PCR assay to decrease rapidly and nonlinearly with decreasing α. As a result, total elimination of probe cross-reactivity (ie, α = 0) is not required to discriminate WT and MT alleles in either a quantitative real-time PCR or ddPCR assay. For example, in the ddPCR assays described here, we find that an α < approximately 0.3 at T_a is sufficient to eliminate a false WT end-point fluorescence signal arising from cross-hybridization of the WT-specific probe. The lack of appreciable end-point fluorescence at α < 0.3 may be related to findings of Holland et al,[46] who reported that during polymerization Taq displaces the first two or so bases it encounters before cleaving at that site. Thus, probe hydrolysis by Taq requires lifting the 5′-end of the probe off of the template. This destabilizes the probe:template duplex such that, when α < 0.3, intact probe release occurs in lieu of fluorescent signal generation, which only occurs if the probe remains duplexed with template through cleavage of the labeled 5′-base.

On the basis of these concepts, a standard pure DNA dual-hydrolysis probe against WT *BRAF* V600 (Table 1) was designed *in silico* with the use of the models of Hughesman et al[39] and SantaLucia[47] to melt at a $T_{m,WT}$ of approximately 66°C to 68°C at ddPCR solution conditions, while also offering the best possible discrimination [$\Delta T_{m,WT-MT_i}$] against all clinically relevant SPMs in codon V600. For that probe, both model-predicted and experimental $\Delta T_{m,WT-MT_i}$ are small (generally ≤ 7°C) for all *BRAF* MT alleles differing from WT *BRAF* by a single SPM within codon V600 (Table 2), reflecting the relatively low proportional contribution of the mismatch to the thermal stability of the cross-hybridization duplex. The consequences of this are reflected in Figure 4A, which overlays ddPCR output data for the WT-negative assay (Figure 2B) sequentially applied to WT *BRAF* and to a representative set of clinically relevant V600 coding mutations presented in the form of purified linearized plasmid DNA. Application of the WT-negative screen against a WT *BRAF* sample generates a tight cluster of droplets displaying a strong FAM^+/HEX^+ signal. For MT alleles that

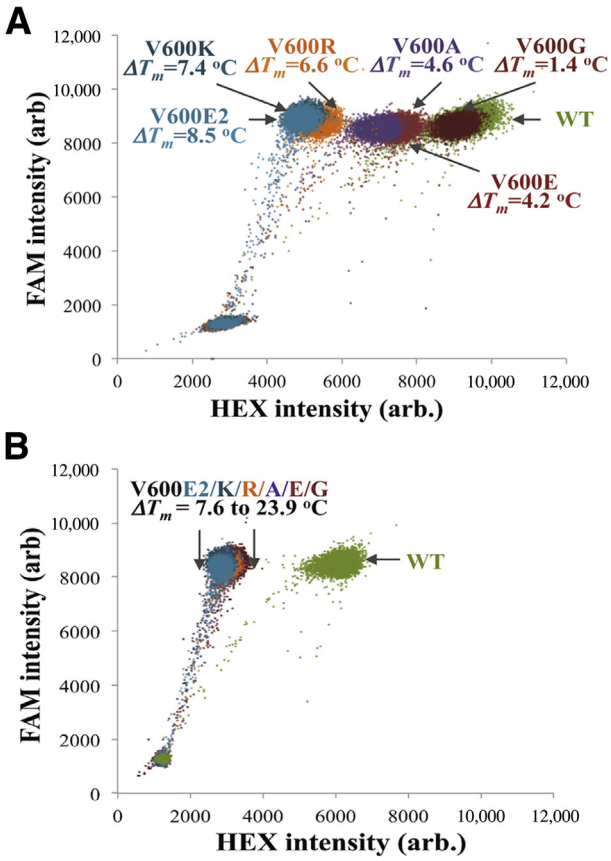

Figure 4 Influence of ΔT_m value on the performance of the WT-negative component of the ddPCR *BRAF* V600 status assay (well 2). Overlay of two-dimensional data output for the WT-negative digital PCR assay (well 2) independently applied against WT *BRAF* and six clinically relevant BRAF V600 MT plasmid DNA samples. **A:** Pure-DNA V600 WT-specific probe: data clusters for assay applied against MT alleles merge with the corresponding data cluster for the WT allele as ΔT_m decreases to values <7°C, as seen for *BRAF* V600E, V600A, and V600G. **B:** LNA V600 WT-specific probe: a ΔT_m >7°C is achieved against every MT allele, resulting in complete segregation of the data cluster for WT *BRAF* from that for every clinically relevant V600 mutation. arb, arbitrary; ddPCR, droplet-digital PCR; FAM, 6-carboxyfluorescein; LNA, locked nucleic acid; MT, mutant; WT, wild-type.

carry two SPMs in codon V600 (eg, $V600E_2$, V600K), $\Delta T_{m,WT-MT_i}$ is sufficiently large that an appreciable HEX^+ signal that results from cross-hybridization of the WT-specific probe is avoided; a tight cluster of FAM^+/HEX^- droplets that show no overlap with the WT *BRAF* cluster is therefore observed. However, for alleles having a single point mutation in codon V600, the MT^+ cluster tends to carry a substantial HEX^+ signal; overlap of WT and MT data clusters is therefore observed for several V600 MTs (G, A, and most significantly E_1), negating the ability to unequivocally discriminate WT and MT V600 alleles. For those cross-reactive MT alleles (Table 2), $\Delta T_{m,WT-MT_i}$ is low (<6°C) and α is > 0.3.

Alternative strategies for achieving suitable $\Delta T_{m,WT-MT_i}$ and α values for each possible V600 coding mutation include chemically modifying the V600 WT-specific probe through either addition of a 3′ terminal minor groove binder ligand[48] or by substituting nucleotides within the probe with their corresponding LNA.[49] We pursued the latter approach. Table 1 reports an LNA-substituted probe against WT *BRAF* V600 designed in the same *in silico* manner to achieve a $\Delta T_{m,WT-MT_i} > 7°C$ and an $\alpha < 0.3$ for all known V600 mutations (Table 2). Use of the LNA/DNA chimeric probe in the WT-negative screen then results in complete segregation of the WT data cluster from all MT data clusters (Figure 4B), permitting

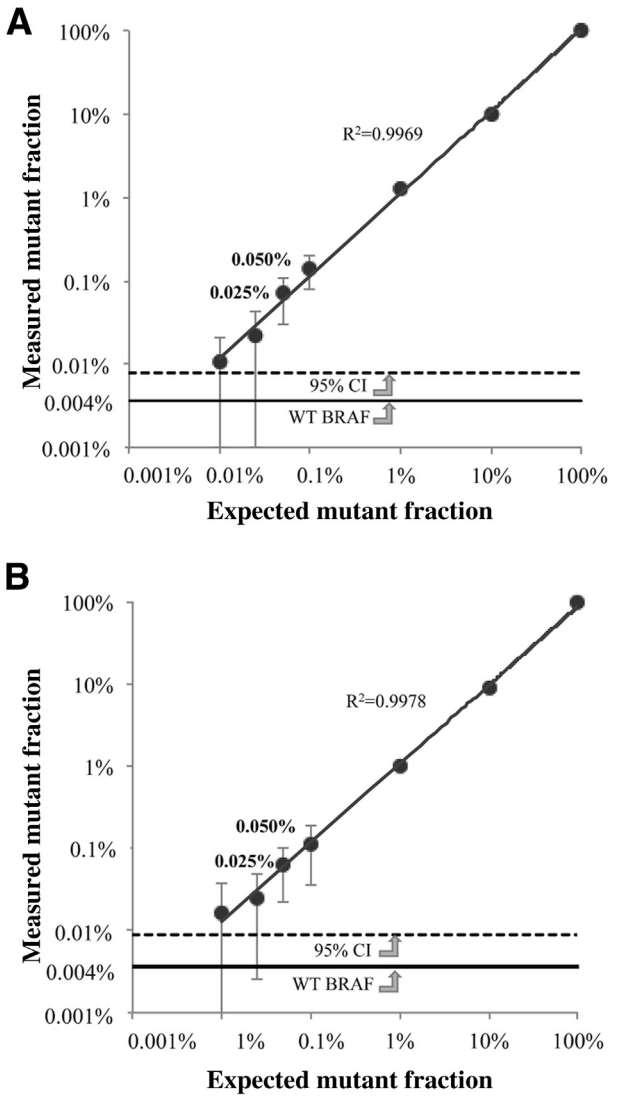

Figure 5 **A** and **B:** Analytical sensitivity (LOD) of the WT-negative component of the ddPCR *BRAF* V600 status assay when applied to plasmid (**A**) and cell-line gDNA (**B**) standards. Measured MF and SD values are plotted versus expected MF for serial dilutions down to 0.01% MF. The **dotted line** is the LOB of the WT-negative component of the assay. Significant linear correlation ($R^2 \geq 0.996$; $P < 0.0001$) between the measured and expected MF is observed down to 0.05% MF. Replicates of *BRAF* V600 WT genomic DNA from the specified source (plasmid or cell line) were used to define mean false-positives (WT *BRAF*, **solid horizontal line**) and SDs, from which the 95% CI was determined and used to define the LOB – 0.008% MF for both systems. $n = 24$ for 0.01% to 0.1% MF data; $n = 4$ for MF > 0.1% data; $n = 24$ replicates of *BRAF* V600 WT gDNA. Statistically significant MF values can be obtained to an LOD of 0.05%. ddPCR, droplet-digital PCR; LOB, limit of blank; LOD, limit of detection; MF, mutant frequency; WT, wild-type.

Table 3 Mean MF and SD ($n = 8$) Values Measured with the Droplet-Digital PCR *BRAF* V600 Status Assay

BRAF Allele	Expected MF (%)	Measured MF, means ± SD (%)
V600E	0.10	0.10 ± 0.05
V600K	0.10	0.14 ± 0.06
V600R	0.10	0.11 ± 0.04
V600D	0.10	0.10 ± 0.08
V600M	0.10	0.09 ± 0.04
V600G	0.10	0.11 ± 0.05
V600A	0.10	0.09 ± 0.05
V600L	0.10	0.10 ± 0.06

Samples having 0.10% MF were generated from mutant and wild-type plasmid DNA. Data for all clinically relevant *BRAF* V600 mutations are shown.

ddPCR, droplet-digital PCR; MF, mutant frequency.

unequivocal detection of a V600 mutation and determination of the MF through MT and WT droplet counts. Design of the $BRAF^{V600E1}$ allele-specific probe used in well 1 of the ddPCR assay followed the same strategy and yielded comparable performance results.

Assay LOD on Plasmid, Cell Line, and FFPE Standards

Serial dilutions ($n \geq 8$ for each dilution) of *BRAF* MT plasmid DNA into *BRAF* WT plasmid DNA to MT frequencies down to 0.01% were used to define the LOD in each reaction well. Because of the greater challenge of creating the probe specificity required in the WT-negative screen, the LOD recorded in well 2 defined the overall LOD for the two-well assay. For serial dilutions of V600K into WT *BRAF* plasmid DNA, a LOD of ≤0.05% MF was recorded (Figure 5A). An equivalent or better LOD was recorded for all other V600 mutations. As a result, when applied to gDNA samples of high quality [minimal chemically or mechanically (eg, shear) induced degradation], the two-well assay can be used to quantify MFs down to 0.1% to a high degree of accuracy (Table 3). MF values were computed by exporting raw ddPCR data (Figure 4) into our custom-designed data analysis software. That algorithm accurately identifies and isolates unique data clusters (eg, MT droplet cluster, WT droplet cluster) with the use of a Gaussian mixture model[50] to set cluster borders in both the HEX and FAM dimensions to either side of the mean of the cluster (Figure 1). Droplets falling outside those limits (rain) are eliminated before MF calculation. The data analysis algorithm is fully automated, and results recorded by it, including computed SDs and CIs, agree quantitatively with manually computed results across the full dynamic range of the assay (0.1% to 100% MF).

As illustrated for $BRAF^{V600K}$ (Figure 5B), the basic metrics of assay performance (LOD, limit of blank, CIs, dynamic range) remain unchanged when applied to serial dilutions of gDNA isolated from the YUMAC cell line (homozygous for $BRAF^{V600K}$) into that from the SW480 cell line (WT *BRAF*). In both calibrations, we observed significant linear correlation ($R^2 \geq 0.996$; $P < 0.0001$) between the expected MF and that determined with the ddPCR assay.

V600 MT frequencies detected in gDNA isolated from FFPE standards (Supplemental Figure S1) carry larger uncertainties. The quality (and often the amplifiable quantity) of target template is generally lower in gDNA prepared from FFPE specimens, leading to an array of possible sequence and PCR artifacts.[51] The heterogeneous cell population comprising tissue samples will also display larger genomic sequence diversity. Replicate ($n = 24$) ddPCR *BRAF* V600 status assay runs on gDNA from the 1.4% *BRAF* V600E FFPE reference standard and gDNA from that standard serially diluted into gDNA from the 100% *BRAF* WT V600 FFPE reference (1%, 0.8%, 0.6%, and 0.4% MT frequencies) were therefore conducted to estimate an LOD for the assay when working on gDNA recovered from FFPE samples as an input. For those replicates, statistically significant V600 WT^{-} calls could be made for MT frequencies of 0.8% (0.77% ± 0.62%) and higher. Evidence of MT template (ie, a distinct MT cluster) could be observed at MT frequencies between 0.8% and 0.4% (Supplemental Figure S1), but the SD in MT template counts was too large to discriminate, for instance, 0.6% and 0.4% MFs. An MF of 0.8% was therefore assigned as the sensitivity of our ddPCR assay when applied to FFPE tissue specimens.

Application to FFPE-Stabilized MLH1-Deficient CRC Tumor Cores

CRC cases were selected from a pool of MLH1-deficient tumors identified by IHC testing as part of the population-based Vancouver Coastal Health Lynch syndrome screening program. Three non−MLH1-deficient cases (no. 3, no. 5, and no. 20) were also included.

gDNA specimens purified from the cohort of 41 tumor samples were subjected to our ddPCR assay, and complete BRAF V600 status results for each specimen are reported in Supplemental Table S1 along with corresponding V600E calls made with the MT-specific IHC VE1 assay. Seventeen of 41 CRC samples tested negative for $BRAF^{V600E}$ by VE1 staining, with a typical negative V600E staining result shown in Figure 6. The remaining 24 samples tested positive for $BRAF^{V600E}$ on the basis of uniform VE1 staining as observed for sample 6 (Figure 6).

All 24 MLH1-deficient tumors that tested positive for $BRAF^{V600E}$ by VE1 staining tested both positive for $BRAF^{V600E1}$ (well 1) and negative for WT (well 2) in the ddPCR assay, confirming the accuracy of both components of our assay against the clinically actionable V600E mutation. In addition, one of the specimens (sample 24) (Figure 6) negative for $BRAF^{V600E}$ by VE1 staining likewise tested negative for $BRAF^{V600E1}$ in well 1 of our ddPCR assay but tested WT negative in well 2, with a recorded MF of 57.4% ± 1.9%. Sanger sequencing results for the amplified template (Figure 6) confirm the patient carries the rare $BRAF^{V600R}$ mutation, highlighting the comprehensive ability

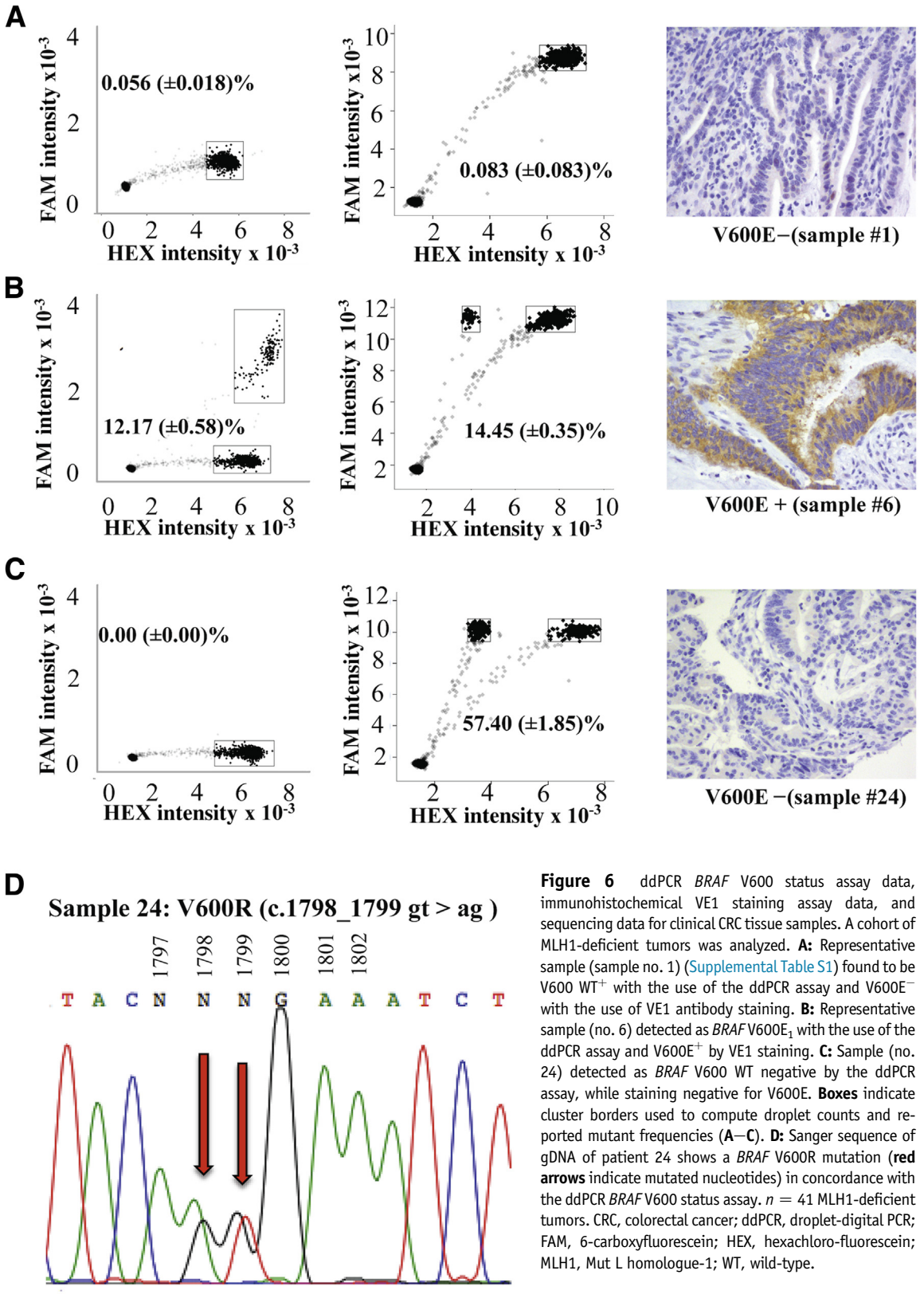

Figure 6 ddPCR *BRAF* V600 status assay data, immunohistochemical VE1 staining assay data, and sequencing data for clinical CRC tissue samples. A cohort of MLH1-deficient tumors was analyzed. **A:** Representative sample (sample no. 1) (Supplemental Table S1) found to be V600 WT^{+} with the use of the ddPCR assay and $V600E^{-}$ with the use of VE1 antibody staining. **B:** Representative sample (no. 6) detected as *BRAF* $V600E_1$ with the use of the ddPCR assay and $V600E^{+}$ by VE1 staining. **C:** Sample (no. 24) detected as *BRAF* V600 WT negative by the ddPCR assay, while staining negative for V600E. **Boxes** indicate cluster borders used to compute droplet counts and reported mutant frequencies (**A**–**C**). **D:** Sanger sequence of gDNA of patient 24 shows a *BRAF* V600R mutation (**red arrows** indicate mutated nucleotides) in concordance with the ddPCR *BRAF* V600 status assay. $n = 41$ MLH1-deficient tumors. CRC, colorectal cancer; ddPCR, droplet-digital PCR; FAM, 6-carboxyfluorescein; HEX, hexachloro-fluorescein; MLH1, Mut L homologue-1; WT, wild-type.

of the ddPCR *BRAF* V600 status assay to both detect clinically relevant V600 mutations and, in the case of rare V600 mutations, provide quantitative evidence that the MF is sufficient to permit unequivocal MT sequence verification.

The remaining 16 specimens that tested negative for $BRAF^{V600E}$ by VE1 staining tested WT positive in the ddPCR assay (Figure 6) on the basis of a mean MF (and error) computed from duplicate runs that fell

below the sensitivity of the assay when applied to FFPE specimens.

Discussion

The growing library of biomarkers prognostic of cancer risk and progression includes somatic mutations in (proto)oncogenes that drive malignant cell proliferation or prolong their survival. Those markers are enabling individual genetic analyses of tumors, which in turn is helping to transform oncology toward the effective design and use of therapeutics against molecular targets and associated signaling-pathway aberrations that are specific to a patient's cancer. Relative to conventional (chemo)-therapeutic treatments, targeted molecular therapies generally offer fewer side effects, can often be administered as a patient-friendly oral dosage, and can prove effective against certain tumor types for which standard therapies offer little to no benefit. The development of panels of biomarkers that offer increasingly detailed pharmacogenetic analyses of patient-specific cancers also points to more comprehensive mutational analyses being used in cancer genetics testing laboratories to facilitate clinical decisions.[52] In the case of an oncogene that is susceptible to either common or more rare somatic mutations in a single codon or adjacent set of codons, this includes assays able to detect the complete set of relevant MT alleles in a manner that not only identifies clinically actionable mutations but also alerts the clinician of a rare mutation that might necessitate more aggressive clinical monitoring by NGS or a personalized course of treatment.

For clinical testing of *BRAF* V600 mutations associated with colorectal cancer, we have shown here how such an assay can be realized by using ddPCR to unambiguously detect $BRAF^{V600E1}$ and thereby identify MLH1-deficient CRC patients unsuitable for anti-EGFR antibody therapy. The assay can further segregate MLH1-deficient tumors into those bearing WT V600 and therefore eligible for treatment with cetuximab or panitumumab and those harboring a rare V600 mutation, for which a more comprehensive NGS-based screen of CRC biomarkers[53] may be justified. Differentiation of WT V600 from MT V600 is achieved with a WT-negative screening strategy, and the assay can be successfully applied to as little as 8 ng gDNA at a total cost of goods of approximately US$8 per sample. Interestingly, the concept of the WT-negative screen has only been described once before, in the landmark paper of Vogelstein and Kinzler[53] that is best known for providing the first description and demonstration of digital PCR. It has not been demonstrated on clinical samples. To our knowledge, the work reported here therefore provides the first evidence that a WT-negative screen can be designed for and successfully applied to mutational analyses of tumor specimens; it therefore adds to a number of powerful new applications of digital PCR to screening of rare alleles.[54,55] Through use of a model-designed LNA/DNA chimeric probe against WT V600, we achieve a sensitivity of 0.8% MF when the assay is applied to gDNA isolated from FFPE specimens. That LOD is dictated by the poorer quality and generally lower quantity of amplifiable *BRAF* template (often 5000 to 8000 copies) that could (and typically can) be extracted from the colorectal FFPE specimens, but nevertheless exceeds that projected for the coming generation of clinical NGS instrumentation ($\geq$1% MF), and is at least 3.5-fold better than that provided by the best NGS technology currently available to clinics. In particular, specific calls on all possible mutations in the *BRAF* V600 codon and proximal codons were achieved by deep pyrosequencing down to MF values $\geq$ 3%.[56] The sensitivity and the mutational coverage of our assay also exceed what can be achieved by conventional IHC testing.

We note that comparable or better sensitivities can be realized with AS PCR assays against a particular MT *BRAF* allele. For example, sensitivities as low as 0.001% were reported in assays against $BRAF^{V600E}$ that used AS quantitative real-time PCR,[57] WT blocking PCR,[58] E-ice-COLD-PCR,[59] or ddPCR.[60] The capabilities of those assays, however, differ considerably from that reported here, because they are not designed to or capable of detecting all *BRAF* V600 mutations. Moreover, they generally do not operate on gDNA recovered from FFPE specimens, for which (as demonstrated in this work) the assay LOD is largely determined by the nature and quantity of amplifiable template available per test.

Finally, some discussion is warranted as to how the ddPCR-based assay described may be extended for application to testing of *BRAF* V600 status in advanced melanomas. The $BRAF^{V600E}$ mutation was accepted as a biomarker predictive of melanoma patient response to the MT B-Raf inhibitors vemurafenib and dabrafenib, whereas a combination of dabrafenib and trametinib was generally accepted for treatment of $V600K^{+}$ metastatic and unresectable melanomas. Multiplexing of the ddPCR assay could permit specific detection of V600E and V600K mutations in well 1. This would require model-based design of a probe against V600K that exhibits no cross-reactivity to WT V600 or any other relevant V600 MT (analogous to the V600E1-specifc probe described in this work). FAM labeling of the V600E-specific probe and, say, Alexa Fluor 488 labeling of the corresponding V600K-specific probe may then be used to unambiguously detect and quantify either mutation in the resulting two-dimensional ddPCR data plot for well 1. Through its ability to detect rare *BRAF* V600 mutations, the WT-negative assay conducted in well 2 could then serve to inform the clinician of the need for enhanced patient monitoring or a more aggressive course of treatment. In this regard, the ability to detect all clinically relevant V600 mutations at frequencies lower than currently achieved by Sanger sequencing or NGS could ameliorate the dangers of a negative sequencing result arising not from absence or remission of disease but rather from a MF below the detection limit of the instrument (approximately 5%). This

concern is heightened by growing evidence that minor subclones positive for a V600 coding mutation have altered immune responses. Moreover, although they typically provide important clinical response over several months, B-Raf inhibitors can alter immune inflammatory mechanisms associated with those aberrant cells. Knowledge of the V600 mutation and the associated immunogenicity of the tumor-associated cells bearing that mutation may therefore provide a sound basis for designing combinations of B-Raf inhibitors and immunotherapeutics that improve progression-free survival by strengthening immune responses or counteracting immune escape mechanisms.[61]

Acknowledgment

Purified gDNA from the SW480 and the YUMAC cell lines was kindly provided by the BC Cancer Agency. Pathological and histological analyses of CRC specimens were performed by Brandon Sheffield and Deanna Johnson, respectively.

Supplemental Data

Supplemental material for this article can be found at *http://dx.doi.org/10.1016/j.jmoldx.2015.09.003*.

References

1. Tomasetti C, Marchionni L, Nowak MA, Parmigiani G, Vogelstein B: Only three driver gene mutations are required for the development of lung and colorectal cancers. Proc Natl Acad Sci U S A 2015, 112: 118−123
2. Alexandrov LB, Nik-Zainal S, Wedge DC, Aparicio SAJR, Behjati S, Biankin AV, et al: Signatures of mutational processes in human cancer. Nature 2013, 500:415−421
3. Nikiforov YE, Nikiforova MN: Molecular genetics and diagnosis of thyroid cancer. Nat Rev Endocrinol 2011, 7:569−580
4. Gazdar AF: Activating and resistance mutations of EGFR in non-small-cell lung cancer: role in clinical response to EGFR tyrosine kinase inhibitors. Oncogene 2009, 28:S24−S31
5. Fakih MG: Metastatic colorectal cancer: current state and future directions. J Clin Oncol 2015, 33:1809−1824
6. Bolton L, Reiman A, Lucas K, Timms J, Cree IA: KRAS mutation analysis by PCR: a comparison of two methods. PLoS One 2015, 10: e0115672
7. Baxter EJ, Scott LM, Campbell PJ, East C, Fourouclas N, Swanton S, Vassiliou GS, Bench AJ, Boyd EM, Curtin N, Scott MA, Erber WN, Green AR; Cancer Genome Project: Acquired mutation of the tyrosine kinase JAK2 in human myeloproliferative disorders. Lancet 2005, 365:1054−1061
8. Marchetti A, Martella C, Felicioni L, Barassi F, Salvatore S, Chella A, Camplese PP, Iarussi T, Mucilli F, Mezzetti A, Cuccurullo F, Sacco R, Buttitta F: EGFR mutations in non-small-cell lung cancer: analysis of a large series of cases and development of a rapid and sensitive method for diagnostic screening with potential implications on pharmacologic treatment. J Clin Oncol 2005, 23: 857−865
9. Loughrey MB, Waring PM, Tan A, Trivett M, Kovalenko S, Beshay V, Young MA, McArthur G, Boussioutas A, Dobrovic A: Incorporation of somatic BRAF mutation testing into an algorithm for the investigation of hereditary non-polyposis colorectal cancer. Fam Cancer 2007, 6:301−310
10. Sensi M, Nicolini G, Petti C, Bersani I, Lozupone F, Molla A, Veggetti C, Nonaka D, Mortarini R, Parmiani G, Fais S, Anichini A: Mutually exclusive NRASQ61R and BRAFV600E mutations at the single-cell level in the same human melanoma. Oncogene 2006, 25: 3357−3364
11. Lasota J, Kowalik A, Wasag B, Wang ZF, Felisiak-Golabek A, Coates T, Kopczynski J, Gozdz S, Miettinen M: Detection of the BRAF V600E mutation in colon carcinoma critical evaluation of the imunohistochemical approach. Am J Surg Pathol 2014, 38:1235−1241
12. Chang YS, Yeh KT, Hsu NC, Lin SH, Chang TJ, Chang JG: Detection of N-, H-, and KRAS codons 12, 13 and 61 mutations with universal RAS primer multiplex PCR and N-, H- and KRAS-specific primer extension. Clin Biochem 2010, 43:296−301
13. Hovelson DH, McDaniel AS, Cani AK, Johnson B, Rhodes K, Williams PD, Bandla S, Bien G, Choppa P, Hyland F, Gottimukkala R, Liu G, Manivannan M, Schageman J, Ballesteros-Villagrana E, Grasso CS, Quist MJ, Yadati V, Amin A, Siddiqui J, Betz BL, Knudsen KE, Cooney KA, Feng FY, Roh MH, Nelson PS, Liu CJ, Beer DG, Wyngaard P, Chinnaiyan AM, Sadis S, Rhodes DR, Tomlins SA: Development and validation of a scalable next-generation sequencing system for assessing relevant somatic variants in solid tumors. Neoplasia 2015, 17:385−399
14. Dumur CI: Available Resources and Challenges for the Clinical Annotation of Somatic Variations. Cancer Cytopathol 2014, 122:730−736
15. Xuan JK, Yu Y, Qing T, Guo L, Shi LM: Next-generation sequencing in the clinic: promises and challenges. Cancer Lett 2013, 340: 284−295
16. Tsongalis GJ, Peterson JD, de Abreu FB, Tunkey CD, Gallagher TL, Strausbaugh LD, Wells WA, Amos CI: Routine use of the Ion-Torrent AmpliSeq (TM) Cancer Hotspot Panel for identification of clinically actionable somatic mutations. Clin Chem Lab Med 2014, 52:707−714
17. Zehir A, Mitchell T, Cheng WJ, Oultache A, Nafa K, Arcila ME, Berger MF, Cheng DT, Hedvat CV: A paired-sample analysis pipeline for removing artifacts in point mutation calls made from the Illumina TruSeq Amplicon Cancer Panel (TSACP) assay. J Mol Diagn 2013, 15:941−942
18. Kinde I, Wu J, Papadopoulos N, Kinzler KW, Vogelstein B: Detection and quantification of rare mutations with massively parallel sequencing. Proc Natl Acad Sci U S A 2011, 108:9530−9535
19. Lou DL, Hussmann JA, McBee RM, Acevedo A, Andino R, Press WH, Sawyer SL: High-throughput DNA sequencing errors are reduced by orders of magnitude using circle sequencing. Proc Natl Acad Sci U S A 2013, 110:19872−19877
20. Davies H, Bignell GR, Cox C, Stephens P, Edkins S, Clegg S, et al: Mutations of the BRAF gene in human cancer. Nature 2002, 417: 949−954
21. Curtin JA, Fridlyand J, Kageshita T, Patel HN, Busam KJ, Kutzner H, Cho KH, Aiba S, Brocker EB, LeBoit PE, Pinkel D, Bastian BC: Distinct sets of genetic alterations in melanoma. N Engl J Med 2005, 353:2135−2147
22. Yip L, Nikiforova MN, Carty SE, Yim JH, Stang MT, Tublin MJ, LeBeau SO, Hodak SP, Ogilvie JB, Nikiforov YE: Optimizing surgical treatment of papillary thyroid carcinoma associated with BRAF mutation. Surgery 2009, 146:1215−1223
23. Vaughn CP, Zobell SD, Furtado LV, Baker CL, Samowitz WS: Frequency of KRAS, BRAF, and NRAS mutations in colorectal cancer. Genes Chromosomes Cancer 2011, 50:307−312
24. Chapman PB, Hauschild A, Robert C, Haanen JB, Ascierto P, Larkin J, Dummer R, Garbe C, Testori A, Maio M, Hogg D, Lorigan P, Lebbe C, Jouary T, Schadendorf D, Ribas A, O'Day SJ, Sosman JA, Kirkwood JM, Eggermont AM, Dreno B, Nolop K, Li J, Nelson B, Hou J, Lee RJ, Flaherty KT, McArthur GA; Brim-3 Study Group: Improved survival with vemurafenib in melanoma with braf v600e mutation. N Engl J Med 2011, 364:2507−2516

25. Flaherty KT, Puzanov I, Kim KB, Ribas A, McArthur GA, Sosman JA, O'Dwyer PJ, Lee RJ, Grippo JF, Nolop K, Chapman PB: Inhibition of mutated, activated BRAF in metastatic melanoma. N Engl J Med 2010, 363:809−819
26. Ravnan MC, Matalka MS: Vemurafenib in patients with BRAF V600E mutation-positive advanced melanoma. Clin Ther 2012, 34: 1474−1486
27. Luke JJ, Hodi FS: Ipilimumab, vemurafenib, dabrafenib, and trametinib: synergistic competitors in the clinical management of BRAF mutant malignant melanoma. Oncologist 2013, 18: 717−725
28. Heinzerling L, Kuhnapfel S, Meckbach D, Baiter M, Kaempgen E, Keikavoussi P, Schuler G, Agaimy A, Bauer J, Hartmann A, Kiesewetter F, Schneider-Stock R: Rare BRAF mutations in melanoma patients: implications for molecular testing in clinical practice. Br J Cancer 2013, 108:2164−2171
29. Rubinstein JC, Sznol M, Pavlick AC, Ariyan S, Cheng E, Bacchiocchi A, Kkluger HM, Narayan D, Halaban R: Incidence of the V600K mutation among melanoma patients with BRAF mutations, and potential therapeutic response to the specific BRAF inhibitor PLX4032. J Transl Med 2010, 8:67
30. Lovly CM, Dahlman KB, Fohn LE, Su Z, Dias-Santagata D, Hicks DJ, Hucks D, Berry E, Terry C, Duke M, Su YJ, Sobolik-Delmaire T, Richmond A, Kelley MC, Vnencak-Jones CL, Iafrate AJ, Sosman J, Pao W: Routine multiplex mutational profiling of melanomas enables enrollment in genotype-driven therapeutic trials. PLoS One 2012, 7:e35309
31. Yang H, Higgins B, Kolinsky K, Packman K, Go Z, Iyer R, Kolis S, Zhao S, Lee R, Grippo JF, Schostack K, Simcox ME, Heimbrook D, Bollag G, Su F: RG7204 (PLX4032), a selective BRAFV600E inhibitor, displays potent antitumor activity in preclinical melanoma models. Cancer Res 2010, 70:5518−5527
32. Di Nicolantonio F, Martini M, Molinari F, Sartore-Bianchi A, Arena S, Saletti P, De Dosso S, Mazzucchelli L, Frattini M, Siena S, Bardelli A: Wild-type BRAF is required for response to panitumumab or cetuximab in metastatic colorectal cancer. J Clin Oncol 2008, 26: 5705−5712
33. Prahallad A, Sun C, Huang S, Di Nicolantonio F, Salazar R, Zecchin D, Beijersbergen RL, Bardelli A, Bernards R: Unresponsiveness of colon cancer to BRAF(V600E) inhibition through feedback activation of EGFR. Nature 2012, 483:100−103
34. Minoo P, Moyer MP, Jass JR: Role of BRAF-V600E in the serrated pathway of colorectal tumourigenesis. J Pathol 2007, 212: 124−133
35. Pietrantonio F, Petrelli F, Coinu A, Di Bartolomeo M, Borgonovo K, Maggi C, Cabiddu M, Iacovelli R, Bossi I, Lonati V, Ghilardi M, de Braud F, Barni S: Predictive role of BRAF mutations in patients with advanced colorectal cancer receiving cetuximab and panitumumab: a meta-analysis. Eur J Cancer 2015, 51:587−594
36. Tufano RP, Teixeira GV, Bishop J, Carson KA, Xing M: BRAF mutation in papillary thyroid cancer and its value in tailoring initial treatment: a systematic review and meta-analysis. Medicine (Baltimore) 2012, 91:274−286
37. Hughesman CB, Turner RFB, Haynes CA: Role of the heat capacity change in understanding and modeling melting thermodynamics of complementary duplexes containing standard and nucleobase-modified LNA. Biochemistry 2011, 50:5354−5368
38. Hughesman C, Fakhfakh K, Bidshahri R, Lund HL, Haynes C: A new general model for predicting melting thermodynamics of complementary and mismatched B-form duplexes containing locked nucleic acids: application to probe design for digital PCR detection of somatic mutations. Biochemistry 2015, 54: 1338−1352
39. Hughesman CB, Turner RF, Haynes C: Correcting for heat capacity and 5'-TA type terminal nearest neighbors improves prediction of DNA melting temperatures using nearest-neighbor thermodynamic models. Biochemistry 2011, 50:2642−2649
40. Untergasser A, Cutcutach I, Koressaer T, Ye J, Faircloth BC, Remm M, Rozen SG: Primer3−new capabilities and interfaces. Nucleic Acids Res 2012, 40:e115
41. Hughesman CB, Turner RFB, Haynes C: Measuring, interpreting and modeling the stabilities and melting temperatures of B-form DNA that exhibits a two-state helix-to-coil transition. Edited by von Stocker U, van der Wielen LAM. Biothermodynamics: The Role of Thermodynamics in Biochemical Engineering. Lausanne, Switzerland, EPFL Press, 2013, pp 355−389
42. Ye J, Coulouris G, Zaretskaya I, Cutcutache I, Rozen S, Madden T: Primer-BLAST: a tool to design target-specific primers for polymerase chain reaction. BMC Bioinformatics 2012, 13:134
43. Benaglia T, Chauveau D, Hunter DR, Young D: Mixtools: an R package for analyzing finite mixture models. J Stat Softw 2009, 32: 1−29. doi:10.18637/jss.v032.i06
44. Halait H, DeMartin K, Shah S, Soviero S, Langland R, Cheng S, Hillman G, Wu L, Lawrence HJ: Analytical performance of a real-time PCR-based assay for V600 mutations in the BRAF gene, used as the companion diagnostic test for the novel BRAF inhibitor vemurafenib in metastatic melanoma. Diagn Mol Pathol 2012, 21: 1−8
45. Tuomi JM, Voorbraak F, Jones DL, Ruijter JM: Bias in the Cq value observed with hydrolysis probe based quantitative PCR can be corrected with the estimated PCR efficiency value. Methods 2010, 50: 313−322
46. Holland PM, Abramson RD, Watson R, Gelfand DH: Detection of specific polymerase chain reaction product by utilizing the 5' to 3' exonuclease activity of Thermus aquaticus DNA polymerase. Proc Natl Acad Sci U S A 1991, 88:7276−7280
47. SantaLucia J Jr, Hicks D: The thermodynamics of DNA structural motifs. Annu Rev Biophys Biomol Struct 2004, 33:415−440
48. Itabashi T, Maesawa C, Uchiyama M, Higuchi T, Masuda T: Quantitative detection of mutant alleles of the K-ras gene with minor groove binder-conjugated fluorogenic DNA probes. Int J Oncol 2004, 24:687−696
49. Denys B, El Housni H, Nollet F, Verhasselt B, Philippe J: A real-time polymerase chain reaction assay for rapid, sensitive, and specific quantification of the JAK2V617F mutation using a locked nucleic acid-modified oligonucleotide. J Mol Diagn 2010, 12:512−519
50. Banfield JD, Raftery AE: Model-based gaussian and non-gaussian clustering. Biometrics 1993, 49:803−821
51. Do HD, Dobrovic A: Sequence artifacts in DNA from formalin-fixed tissues: causes and strategies for minimization. Clin Chem 2015, 61: 64−71
52. Kim RY, Xu H, Myllykangas S, Ji H: Genetic-based biomarkers and next-generation sequencing: the future of personalized care in colorectal cancer. Per Med 2011, 8:331−345
53. Vogelstein B, Kinzler KW: Digital PCR. Proc Natl Acad Sci U S A 1999, 96:9236−9241
54. Castellanos-Rizaldos E, Paweletz C, Song C, Oxnard GR, Mamon H, Jänne PA, Makrigiorgos GM: Enhanced ratio of signals enables digital mutation scanning for rare allele detection. J Mol Diagn 2015, 17:284−292
55. Lamy PJ, Castan F, Lozano N, Montélion C, Audran P, Bibeau F, Roques S, Montels F, Laberenne AC: Next-generation genotyping by digital PCR to detect and quantify the BRAF V600E mutation in melanoma biopsies. J Mol Diagn 2015, 17:366−373
56. Skorokhod A, Helmbold P, Brors B, Schirmacher P, Enk A, Penzel R: Automated universal BRAF state detection within the activation segment in skin metastases by pyrosequencing-based assay U-BRAF(V600). PLoS One 2013, 8:e59221
57. Szankasi P, Reading NS, Vaughn CP, Prchal JT, Bahler DW, Kelley TW: A quantitative allele-specific PCR test for the BRAF V600E mutation using a single heterozygous control plasmid for quantitation: a model for qPCR testing without standard curves. J Mol Diagn 2013, 15:248−254

58. Chen D, Huang JF, Xia H, Duan GJ, Chuai ZR, Yang Z, Fu WL, Huang Q: High-sensitivity PCR method for detecting BRAF V600E mutations in metastatic colorectal cancer using LNA/DNA chimeras to block wild-type alleles. Anal Bioanal Chem 2014, 406: 2477−2487
59. How-Kit A, Lebbé C, Bousard A, Daunay A, Mazaleyrat N, Daviaud C, Mourah S, Tost J: Ultrasensitive detection and identification of BRAF V600 mutations in fresh frozen, FFPE, and plasma samples of melanoma patients by E-ice-COLD-PCR. Anal Bioanal Chem 2014, 406:5513−5520
60. Sanmamed MF, Fernández-Landázuri S, Rodriguez C, Zárate R, Lozano MD, Zubiri L, Perez-Gracia JL, Martin-Algarra S, González A: Quantitative cell-free circulating BRAFV600E mutation analysis by use of droplet digital PCR in the follow-up of patients with melanoma being treated with BRAF inhibitors. Clin Chem 2015, 61:297−304
61. Ilieva KM, Correa I, Josephs DH, Karagiannis P, Egbuniwe IU, Cafferkey MJ, Spicer JF, Harries M, Nestle FO, Lacy KE, Karagiannis SN: Effects of BRAF mutations and BRAF inhibition on immune responses to melanoma. Mol Cancer Ther 2014, 13: 2769−2783